

# Chaos controlled and disorder driven phase transitions induced by breaking permutation symmetry

Manju C,<sup>1,\*</sup> Arul Lakshminarayan,<sup>2,†</sup> and Uma Divakaran<sup>1,‡</sup>

<sup>1</sup>*Department of Physics, Indian Institute of Technology Palakkad, Kerala, 678623.*

<sup>2</sup>*Department of Physics, & Center for Quantum Information, Computation and Communication, Indian Institute of Technology Madras, Chennai, India 600036*

(Dated: September 23, 2024)

The effects of disorder and chaos on quantum many-body systems can be superficially similar, yet their interplay has not been sufficiently explored. This work finds a continuous phase transition when disorder breaks permutation symmetry, with details of the transition being controlled by the degree of chaos in the clean limit. The system changes from an area law entangled phase in the permutation symmetric subspace where collective variables exist to volume law entanglement in the full Hilbert space, beyond a critical strength of the disorder. The critical strength tends to zero when the original disorder free system is fully chaotic. We study this mainly via the scaling of the collective spin of non-equilibrium states which transit to have properties of what has been dubbed “deep Hilbert space”. This has potential implications for general many body physics, as well as technologies such as transmon qubits.

## I. INTRODUCTION

Deterministic chaos, originating in the lack of sufficient number of conserved quantities, gives rise to ergodic and mixing dynamics with a positive Lyapunov exponent in the classical case [1–3], and in the quantum case results in states with random matrix properties, thermalization and volume law entanglement [4–11]. Disorder, depending on its relative strength on the other hand, can lead to Griffiths phases [12], Anderson [13] or many-body localization [14, 15], and can also result in thermalization and delocalization via breaking symmetries. For example, the extensively investigated Sachdev-Ye-Kitaev (SYK) model, related to the physics of quantum black holes, is one where randomized all-to-all couplings results in maximal quantum chaos [16–18]. Deterministic chaos can sometimes be modeled as being pseudo-random and insights from disorder physics can be applied as in the well-known connection between dynamical and Anderson localization [19].

Arrays of superconducting Josephson junction based transmons, which are nonlinear oscillators, are currently the most successful implementations of quantum computers [20–22]. Disorder in the energies of the individual qubit transmons is a necessary evil in the presence of inter-transmon couplings. A detailed study of the consequences for these devices comes with a warning of being “dangerously close to a phase of uncontrollable chaotic fluctuations” [23]. It has also long been appreciated that dynamical chaos has serious effects on practical implementation of quantum many-body systems, as it can increase entanglement to random state values, and small subsystems face effective decoherence, thus questioning

the reliability of quantum information processing [24–36]. For example, it has been discussed in Ref. [30] that the presence of random individual qubit energies along with residual short range interactions can make the system chaotic under certain limits that compromises the quantum computer losing its ability to perform well.

Classically it was also found that disorder can “tame” chaos, wherein nonlinear oscillators get synchronized from a chaotic phase in the presence of disorder [37]. Similarly, many-body localization takes the system from an ergodic phase to a localized one by increasing disorder [15, 38–40]. It is thus desirable to study the effects of disorder in systems which have a well-established regular  $\rightarrow$  chaotic route in the semiclassical or mean-field limit. Here, the transitions in physical properties whose origins lie in dynamical chaos and those from disorder are both at play together.

Towards this end, we investigate the dynamics of  $N$  particles originally restricted to the small  $O(N)$  permutation symmetric subspace (PSS), but that can have various dynamical regimes, from near-integrable to intermediate and fully chaotic. The disorder breaks the permutation symmetry and results in a phase transition into the full exponentially large,  $O(\exp(N))$  Hilbert space. Interestingly, the extent of chaos in the “clean” symmetric space is found to dictate the critical strength of the disorder that ensures the dynamics has penetrated to the full Hilbert space (FHS), in the large  $N$  limit. The transition has many possible order parameters. The block entanglement changes from area law  $\sim \ln N$ , characteristic of permutation symmetric states [41] to volume law  $\sim N$ . Collective observables such as the total angular momentum changes from  $\sim N$  to  $\sim \sqrt{N}$ . This transition thus shows similarities to a superradiant to radiant phases of collective atomic states in a cavity [42–44]. Recent studies have explored the effect of introducing non-uniform initial states on the dynamics of a permutation symmetric Hamiltonian [45, 46] which can go into the “deep Hilbert space” [45], defined as states whose total

\* 222004003@smail.iitpkd.ac.in

† arul@physics.iitm.ac.in

‡ uma@iitpkd.ac.in

angular momentum scales as  $\sqrt{N}$ .

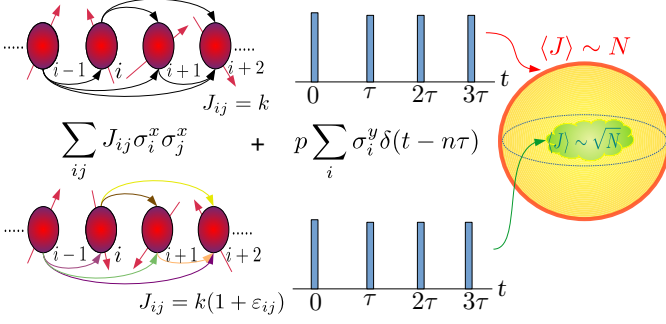


FIG. 1. Schematic of the dynamics: Top row corresponds to the disorder free system where interactions connecting different spins have same magnitude  $J_{ij} = k$ . The second term of the Hamiltonian is the periodic kicks along  $y$ -direction in uniform magnetic fields. Bottom row corresponds to a disordered system where  $J_{ij}$  are random. The angular momentum sphere on the right is a caricature of states with  $\langle J \rangle$  for the disorder free system restricted on the surface of this sphere, whereas for the disordered system it is pushed inside the sphere where  $\langle J \rangle \sim \sqrt{N}$ .

## II. THE MODEL

A convenient model to study the interplay of chaos and disorder is provided by the kicked top which is a textbook example of quantum chaos [47–49], consisting of one large spin of angular momentum  $S = N/2$ , that can be considered as the collective dynamics of  $N$  spin  $1/2$  particles within the permutation symmetric subspace [50, 51]. Several experiments have fruitfully implemented this to understand the effects of chaos on entanglement [52–54].

A disordered version of the kicked top can be used to investigate the effects of breaking permutation symmetry. The specific Hamiltonian that we study is given by

$$H = \frac{k}{2N\tau} \sum_{\ell < \ell'=1}^N (1 + \epsilon_{\ell\ell'}) \sigma_{\ell}^x \sigma_{\ell'}^x + \frac{p}{2} \sum_{n=-\infty}^{\infty} \sum_{\ell=1}^N \sigma_{\ell}^y \delta(t - n\tau), \quad (1)$$

where,  $\sigma_{\ell}^{\nu}$  with  $\nu = x, y, z$  are the Pauli matrices at site  $\ell$ , and  $k$  is the interaction strength that can be tuned such that there is a transition from regular to deterministic chaotic dynamics in the disorder free Hamiltonian,  $\tau$  is the time period of delta kicks that is set to unity, and  $p$  is fixed to  $\pi/2$  to compare with the known results. Here,  $\epsilon_{\ell\ell'}$  are the random (quenched disorder) part of the spin interactions taken from a normal distribution with zero mean and standard deviation  $w$ , also referred to as disorder strength. The corresponding unitary Floquet operator  $U_w$  that evolves states infinitesimally be-

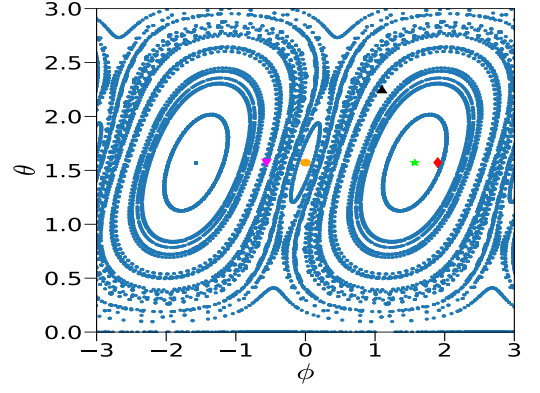


FIG. 2. Classical map of kicked top for  $k = 1$ . The points highlighted in various colors correspond to different initial conditions  $(\theta, \phi)$  studied in this work, namely,  $\blacktriangle = (2.25, 1.1)$ ,  $\bullet = (\pi/2, 0)$ ,  $\star = (\pi/2, \pi/2)$ ,  $\blacktriangledown = (\pi/2, -0.56)$ ,  $\blacklozenge = (\pi/2, 1.9)$ .

fore consecutive kicks separated by the period  $\tau$ , is given by

$$\exp \left( -i \frac{k}{2N} \sum_{\ell < \ell'=1}^N (1 + \epsilon_{\ell\ell'}) \sigma_{\ell}^x \sigma_{\ell'}^x \right) \exp \left( -i \frac{\pi}{4} \sum_{\ell=1}^N \sigma_{\ell}^y \right), \quad (2)$$

where we have set  $\hbar = 1$ . A schematic diagram of the Hamiltonian studied is shown in Fig. 1.

The disorder free version  $U_0$ , with all  $\epsilon_{\ell\ell'} = 0$ , is the quantum kicked top [7, 36, 47, 49, 55–67] where the Hamiltonian is purely a function of the collective spin operators  $J_{\alpha} = \sum_{\ell}^N \sigma_{\ell}^{\alpha}/2$  where  $\alpha = x, y, z$ . The total angular momentum  $J^2 = J_x^2 + J_y^2 + J_z^2$  defined in terms of these collective spins is a constant of motion in the quantum kicked top [49, 50, 68]. Various aspects of disorder free long range interacting systems such as the one given above are discussed in Ref. [69–71]. The large  $N$  limit of  $U_0$  is studied as a symplectic classical map on the unit sphere  $(X, Y, Z) \mapsto (X', Y', Z')$  where  $X = J_x/J$ ,  $Y = J_y/J$  and  $Z = J_z/J$ . This map shows regular dynamics for small values of  $k$ , typically  $< 2$ , and fully chaotic dynamics for large values of  $k$  ( $k > 6$ ), where the Lyapunov exponent may be approximated as  $(\ln k - 1)$  [72, 73]. The Heisenberg evolution equations of the angular momentum operators are given by:

$$\langle J_i \rangle_{n+1} = \langle U^{\dagger} J_i U \rangle_n. \quad (3)$$

The classical equations of motion can be obtained in the limit  $j \rightarrow \infty$ , and are given by :

$$\begin{aligned} X_{n+1} &= Z_n, \\ Y_{n+1} &= Y_n \cos(kZ_n) + X_n \sin(kZ_n), \\ Z_{n+1} &= -X_n \cos(kZ_n) + Y_n \sin(kZ_n). \end{aligned} \quad (4)$$

The classical phase space map for  $k = 1$  is shown in Fig. 2, where  $(\theta, \phi)$  corresponds to the spherical coordinates of the total angular momentum, showing a predominantly regular behavior at this parameter value.

In the quantum case, one can initialize the system in a spin coherent state given by [74–76]

$$|\psi_0\rangle = |\theta, \phi\rangle = \left( \cos \frac{\theta}{2} |0\rangle + e^{i\phi} \sin \frac{\theta}{2} |1\rangle \right)^{\otimes N}. \quad (5)$$

It corresponds to a localized state around the classical point  $(X, Y, Z) = (\sin \theta \cos \phi, \sin \theta \sin \phi, \cos \theta)$ . The quantum state after  $n$  Floquet periods is  $|\psi_n\rangle = U_0^n |\psi_0\rangle$ . The states at all times  $n$  are restricted to the  $N + 1$  dimensional PSS and conserve the total angular momentum  $J^2 = (N/2)(N/2 + 1)$ . It has also been shown that the chaotic phase can be described using a random matrix theory (RMT) in  $N + 1$  dimensions [49]. For small values of  $N (\leq 4)$ , the kicked top is exactly solvable and does yield interesting insights already into the large  $N$  cases [77–79].

Introducing disorder in the system will break the permutation symmetry of the Hamiltonian, and the state  $|\psi_n\rangle$  after  $n$  kicks given by  $U_w^n |\psi_0\rangle$  will now be out of PSS where  $J^2$  is no longer a constant of motion. If the state  $|\psi_n\rangle$  in the presence of large disorder tends to a random state on the full Hilbert space, denoted as  $|\psi_{\text{RMT}}\rangle$ , the expectation value of  $J_z^2$  can be estimated as:

$$\langle J_z^2 \rangle_{\text{RMT}} = \sum_{j=1}^{2^N} \lambda_j^2 |\langle \psi_{\text{RMT}} | \phi_j \rangle|^2 = N/4, \quad (6)$$

where  $|\phi_j\rangle = |j_1 \dots j_N\rangle$ ,  $j_i = \pm 1$ , are eigenvectors of  $J_z$  with eigenvalues  $\lambda_j = (\sum_\ell j_\ell)/2$ . The ensemble average over random states  $|\langle \psi_{\text{RMT}} | \phi_j \rangle|^2 = 1/2^N$  is used above along with the fact that  $\text{Tr } J_z^2 = N2^{N-2}$ . Similarly  $\langle J_x^2 \rangle_{\text{RMT}} = \langle J_y^2 \rangle_{\text{RMT}} = N/4$ , and hence  $\langle J^2 \rangle_{\text{RMT}} = 3N/4$ . Clearly,  $\langle J^2 \rangle$  exhibit a change in the scaling when the dynamics shifts from the permutation symmetric subspace where  $\langle J^2 \rangle \sim N^2$  to the FHS where the state being close to random has a  $\sim N$  scaling. It is this transition of the dynamics to the “full” Hilbert space that we shall focus in the current work.

One can also capture this change in the dynamics by studying von Neumann entropy  $S_Q(A)$  of the subsystem  $A$  consisting of  $Q$ – spins or qubits. The von Neumann entropy is given by  $S_Q(A) = -\text{tr}(\rho_A \log_2 \rho_A)$ , where  $\rho_A$  is the reduced density matrix of subsystem  $A$ . The expression for  $S_Q(A)$  using ensemble averaging over random permutation symmetric states is approximated by [41]

$$\langle S_Q(A) \rangle_{\text{PSS}} \approx \log_2(Q + 1) - \frac{2}{3} \left( \frac{Q + 1}{N - Q + 1} \right). \quad (7)$$

We have checked numerically that  $S_Q(A)$  even in the regular regime of small  $k$  within permutation symmetric subspace is proportional to  $\log_2(Q + 1)$ . A related work calculating the von Neumann entropy in PSS is given in Ref.[80]. On the other hand, when the dynamics traverse the full Hilbert space,  $S_Q(A)$  is given by the Page value [38, 41, 81]:

$$\langle S_Q(A) \rangle_{2^Q} \approx Q - \frac{1}{\ln 2} \left( \frac{2^Q}{2^{N-Q+1}} \right). \quad (8)$$

Thus, we conclude that as the disorder strength  $w$  is increased, various expectation values will potentially shift from their values within the permutation symmetric subspace to the RMT values relevant to the full Hilbert space. This is because increasing the strength of the disorder  $w$  will not only take the system out of the permutation symmetric subspace but will also make it more chaotic since increasing  $w$  is equivalent to increasing  $k$  as can be seen from Eq. 1. Below, we substantiate these change in scalings of  $J^2$  and  $S_Q(A)$  using numerics.

### III. RESULTS AND DISCUSSIONS

It is both instructive and interesting to first examine the evolution of the model in Eq. 1 without the periodic kicks ( $p = 0$ ). This is the well-known spin-glass model, the Sherrington-Kirkpatrick model [82–84], with a nonzero average interaction strength. The thermodynamics of this model has long been of great interest. The time evolution of disorder averaged  $\langle J^2(t) \rangle = \langle \psi_t | J^2 | \psi_t \rangle = \langle \psi_t | J_x^2 | \psi_t \rangle + \langle \psi_t | J_y^2 | \psi_t \rangle + \langle \psi_t | J_z^2 | \psi_t \rangle$  for an arbitrary initial coherent state can be solved exactly. Since  $J_x^2$  commutes with the  $p = 0$  Hamiltonian,

$$\langle \psi_t | J_x^2 | \psi_t \rangle = \langle \theta, \phi | J_x^2 | \theta, \phi \rangle = \frac{N}{4} + \frac{N(N-1)}{4} \cos^2 \phi \sin^2 \theta.$$

The calculation of  $\langle \psi_t | (J_y^2 + J_z^2) | \psi_t \rangle$  is more involved. However, a detailed analysis leads to:

$$\begin{aligned} \langle \psi_t | (J_y^2 + J_z^2) | \psi_t \rangle &= \frac{2N}{4} + \frac{N(N-1)}{4} (1 - \cos^2 \phi \sin^2 \theta) \\ &\left[ \int_{-\infty}^{\infty} \frac{1}{\sqrt{2\pi w^2}} \cos \left( \frac{kt}{N} \epsilon_{ij} \right) \exp \left( -\frac{\epsilon_{ij}^2}{2w^2} \right) d\epsilon_{ij} \right]^{2(N-2)} \\ &= \frac{2N}{4} + (1 - \cos^2 \phi \sin^2 \theta) \exp \left[ -w^2 k^2 t^2 (N-2)/N^2 \right], \end{aligned}$$

and hence finally

$$\begin{aligned} \langle J^2(t) \rangle &= \frac{3N}{4} + \frac{N(N-1)}{4} [\cos^2 \phi \sin^2 \theta + \\ &(1 - \cos^2 \phi \sin^2 \theta) \exp \left[ -w^2 k^2 t^2 (N-2)/N^2 \right]]. \end{aligned} \quad (9)$$

Clearly, for a generic initial coherent state,  $\langle J^2(t) \rangle$  decreases exponentially with time and saturates to a disorder independent, but initial state dependent value, which is  $O(N^2)$ . The irreversible nature of the dynamics arises from the disorder averaging even in finite systems. When  $\theta = \pi/2$  and  $\phi = 0$  or  $\pi$ , there is no decay and  $\langle J^2(t) \rangle = \langle J^2(0) \rangle = j(j+1)$ , where  $j = N/2$ . These special initial states have no evolution except for a phase as they are eigenstates of the Hamiltonian. Interestingly, when  $\phi = \pm\pi/2$  (any value of  $\theta$ ),  $\langle J^2(n) \rangle$  saturates to the RMT value given by  $3N/4$  for any non-zero value of disorder. These initial states are in the  $y-z$  plane of the Bloch sphere, and are maximally *coherent* (in the sense of quantum information theory, as discussed below) in the

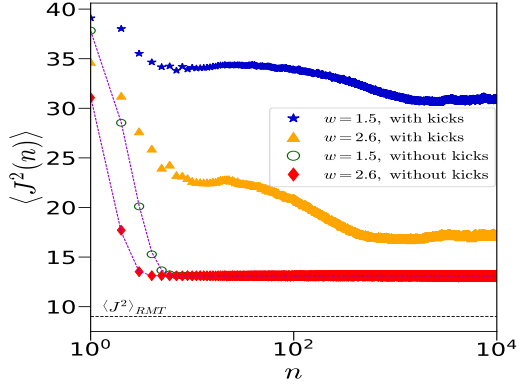


FIG. 3. Evolution of  $\langle J^2(n) \rangle$  with time  $n$  for the disordered system with and without kicks for two different values of disorder strength  $w = 1.5, 2.6$ , initial state  $|\theta, \phi\rangle = |2.25, 1.1\rangle$ ,  $k = 1$ , and  $N = 12$ . The points correspond to numerical data and the dotted lines correspond to the analytical expression given in Eq. 9 for the unkicked Hamiltonian. The black horizontal line is  $\langle J^2_{RMT} \rangle = 3N/4 = 9$  which is well below the saturation value. This saturation value clearly is independent of the strength of disorder, but depends on the initial state, as also predicted by Eq. 9.

preferred  $x$  basis as this is the direction of the interaction. These are the only initial states for which the saturation value of  $J^2$  scales linearly as  $N$ , rather than quadratically, and are unstable in the sense that any deviation in the  $\phi$  value changes this from the RMT scaling. We will find that in the presence of the transverse field kicks when  $p \neq 0$ , these behaviours are interestingly modified, while some persist. Below, we present our results in the presence of kicks, first for a generic coherent state and then for a non-generic, initial coherent states.

### A. A generic initial state

We present the results of numerical calculations which are performed with an initial state  $|\psi_0\rangle$  in the PSS as given in Eq. 5 with  $\theta = 2.25$ ,  $\phi = 1.1$  ( $\blacktriangle$  in Fig. 2) and is evolved to  $|\psi_n\rangle = U_w^n |\psi_0\rangle$  using the Floquet operator  $U_w$  given in Eq. 2. This initial state is “generic” in the sense that it has no special dynamical significance in the permutation symmetric classical limit. It is still a coherent state and not generic in the sense of Haar measure. We use the fast Walsh Hadamard transform to reach system sizes of  $N = 16$ . Fig. 3 compares the dynamics of the system, both, in the absence and in the presence of kicks for two different values of  $w$ . We find that in the absence of kicks, and for the generic initial coherent state when  $\cos \phi \neq 0$ , the system reaches its saturation value when time  $t > t^* \sim \frac{\sqrt{N}}{wk}$  in the large  $N$  limit, which is much smaller than that in the presence of kicks. The relevant time scales in the presence of disorder and kicks is more clearly shown in Fig. 4 using  $\langle J^2(n) \rangle$  and  $S_{N/2}(A)$  for  $k = 1$ . In contrast to the unkicked model, there is a

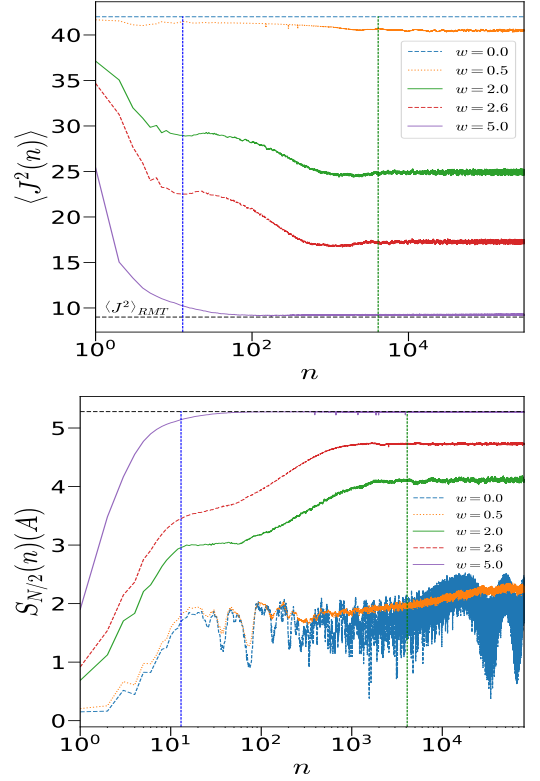


FIG. 4. Top:  $\langle J^2 \rangle$  as a function of number of kicks  $n$  for different disorder strengths  $w$  with  $k = 1$ ,  $N = 12$  qubits, averaged over 100 disorder realizations. Bottom: shows the von Neumann entanglement entropy  $S_{N/2}$  as a function of  $n$  for the same parameters. The two vertical lines correspond to the two Heisenberg time scales discussed in the text,  $t_{PSS}^H$  (blue) and  $t_{FHS}^H$  (green). The black dashed horizontal line in both figures correspond to the RMT values in full Hilbert space.

disorder dependent steady state value eventually reached for all values of the disorder; however we find an interesting feature consisting of two regimes, first is till time  $n \sim t_{PSS}^H = N + 1$  corresponding to the Heisenberg time relevant to the PSS, when there is a quasi steady state value. The other is at  $n \sim t_{FHS}^H = 2^N$ , the Heisenberg time relevant to the FHS where  $\langle J^2 \rangle$  and  $S_{N/2}(A)$  again starts saturating, which implies that the system has “realized” the presence of the full Hilbert space. Notice that with large disorder strength such as  $w = 5$ , when the full Hilbert space is being accessed, the time scale at  $t_{FHS}^H$  has become irrelevant for this quantity. Instead the Heisenberg time for the PSS provides a time scale for thermalization, when  $\langle J^2(n) \rangle$  and  $S_{N/2}(A)$  saturates close to the RMT value corresponding to FHS. This is to be expected as the Heisenberg time for the PSS is also the Ehrenfest or log-time for the dynamics in the FHS. For intermediate values of the disorder strength  $w$ , the nonequilibrium state’s  $J^2$  as well as the entanglement saturates to non-thermal (non-RMT) values, signifying some kind of localization. It would be interesting to com-



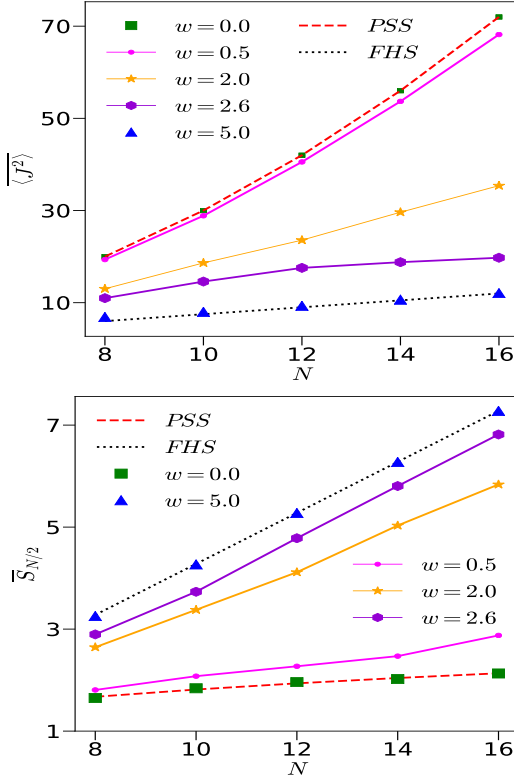


FIG. 5. Top: Change in scaling of  $\overline{\langle J^2 \rangle}$  from  $N^2/4 + N/2$  (red dashed line) to  $3N/4$  (black dotted line) as  $w$  is increased with  $k$  set to 1. Bottom: Same for  $\overline{S}_{N/2}$  as a function of  $N$  at  $k = 1$  where the red dashed line corresponds to fitted line  $0.41 + 0.54 \log_2(N/2 + 1)$  and the black dotted line is the RMT expression given by  $N/2 - 1/2 \ln 2$ .

pare these with the well-studied case of MBL [15, 39, 40].

To quantify the saturation value as a function of the disorder and system size, we now study the behavior of long time averaged values (averaged from  $n = 10^5$  to  $n = 3 \times 10^5$ ) of  $J^2$  and  $S_{N/2}(A)$ , denoted as  $\overline{\langle J^2 \rangle}$  and  $\overline{S}_{N/2}$ , respectively. From the discussions above, we expect that as  $w \rightarrow 0$  or small when the dynamics is predominantly within the permutation symmetric subspace, the scaling of long time limit of various quantities will follow the PSS scaling, *i.e.*,  $\overline{\langle J^2 \rangle} \sim N^2$  and  $\overline{S}_{N/2} \sim \log_2(N/2 + 1)$ . In the other extreme limit, when  $w \rightarrow \infty$  and the dynamics is described by RMT in the full  $2^N$ -dimensions,  $\overline{\langle J^2 \rangle} = 3N/4$  and  $\overline{S}_{N/2} \sim N/2$ . Fig. 5 highlights the above discussed change in scaling when  $w$  is increased. Note that for the solvable case in the absence of kicks, while Eq. 9, indicates an earlier saturation time scale  $\sim \sqrt{N}$  for generic initial coherent states, the saturation value itself is still similar to the PSS case with  $\langle J^2 \rangle \sim N^2$ .

It is tempting to associate this shift in the scaling of  $\overline{\langle J^2 \rangle}$  and  $\overline{S}_{N/2}$  with a second order phase transition. Therefore, we now investigate the possible existence of a critical  $w_c$  below which the dynamics is predominantly within the PSS and above which the dynamics captures the properties of the FHS described by RMT, and obtain

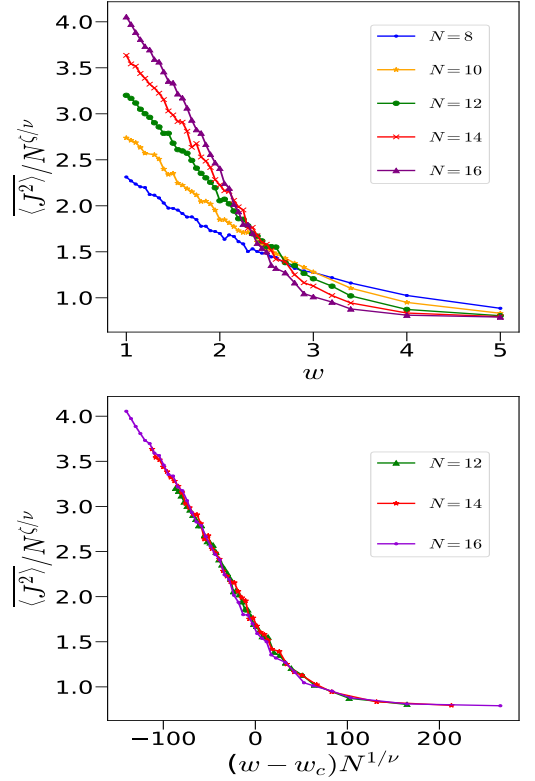


FIG. 6. (Top):  $\overline{\langle J^2 \rangle} / N^{\zeta/\nu}$  as a function of disorder strength  $w$  at  $k = 1$  for different system sizes. These curves cross each other at  $w = w_c \approx 2.38$ . (Bottom): The collapse of the data with  $\zeta = 0.59$  and  $\nu = 0.60$  consistent with the scaling proposed in Eq. 10.

relevant critical exponents of the associated phase transition, if any. We propose a finite size scaling of the form [38, 85–89]

$$\overline{\langle J^2 \rangle} = N^{\zeta/\nu} F((w - w_c)N^{1/\nu}), \quad (10)$$

where  $\nu$  is the correlation length exponent. Fig. 6 (top) shows the crossing of the data around  $w_c = 2.38$  when  $k = 1$  whereas the collapse of the data with  $\nu = 0.60$  and  $\zeta = 0.59$  is shown in Fig. 6 (bottom). In order to confirm this phase transition further, we repeat the calculations for other values of  $k$ , the results of which are shown in Figure 7. It is to be noted that  $k = 4$  is a mixed phase space with considerable chaos already present in the system.

Table I lists the critical disorder strength  $w_c$  along with the critical exponents  $\nu$  and  $\zeta$  for different values of the interaction strength or chaos parameter  $k$ . Intuitively, the chaotic dynamics at larger  $k$  values will require smaller disorder to take the dynamics to the full Hilbert space, which is also what we observe. Interestingly, we also find a weak parameter dependence on the critical exponent  $\nu$  for this phase transition. The exponent  $\nu$  lies within a range of 0.6 to 0.3 for the parameters studied. Such a variation seems to be a characteristic of a finite size disordered system such as the well studied

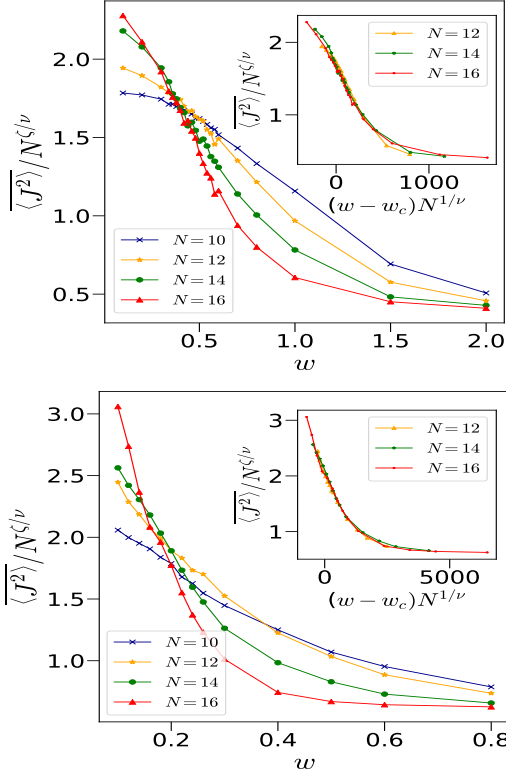


FIG. 7. (Top): The main figure shows the data corresponding to different system sizes for  $k = 2$  crossing each other at  $w = w_c \sim 0.41$  whereas the inset shows the collapse of the data with  $\nu = 0.40$  and  $\zeta = 0.49$ . (Bottom): Same as above but for  $k = 4$  with  $w = w_c \sim 0.17$ ,  $\nu = 0.3$  and  $\zeta = 0.32$ .

many-body-localization [90]. We also find that in most cases,  $\nu \sim \zeta$ . The quality of the data collapse for different values of  $k$  confirm the presence of a second order phase transition. At the same time, we do observe that identifying correct  $w_c$  values for larger  $k$  is difficult since  $w_c$  then is very small and a single crossing point for all system sizes is difficult to obtain. On the other hand when  $k \rightarrow 0$ , the dynamics can get highly non-ergodic and these parameters need more careful examinations. We have further confirmed this phase transition using the entanglement entropy  $\bar{S}_{N/2}$  with a similar finite size scaling given in Eq. 10 resulting to  $\nu = 0.67$ ,  $\zeta = 0.76$  and  $w_c = 1.8$  when  $k = 1$ , as shown in Fig. 8. We do acknowledge the fact that these numerics are limited by finite size systems and may not fully capture the behavior in the thermodynamic limit. This may also be the reason for slightly different values of  $w_c$  obtained using  $\bar{S}_{N/2}$  and  $\langle J^2 \rangle$ .

It is also observed that the collapse is relatively good when the clean system is either predominantly chaotic or predominantly regular. For a mixed phase space, with significant fraction of both regular and chaotic regions, say at  $k = 3$ , the quality of the scaling seems to depend on the initial state. The value in the table I for  $k = 3$  and  $k = 4$  corresponds to chaotic regions. For regular

$k$	$w_c$	$\nu$	$\zeta$
0.5	$3.17 \pm 0.13$	$0.59 \pm 0.04$	$0.63 \pm 0.07$
1.0	$2.38 \pm 0.04$	$0.60 \pm 0.02$	$0.59 \pm 0.06$
2.0	$0.41 \pm 0.01$	$0.40 \pm 0.01$	$0.49 \pm 0.09$
3.0	$0.31 \pm 0.03$	$0.62 \pm 0.06$	$0.87 \pm 0.05$
4.0	$0.17 \pm 0.02$	$0.30 \pm 0.05$	$0.32 \pm 0.05$

TABLE I. Critical disorder strength and exponents  $\nu$ ,  $\zeta$  for different chaos parameter,  $k$ . We have used  $\langle J^2 \rangle$  with  $N = 12, 14$  and  $16$  to identify the critical points with time averaging ranging from  $n = 10^5$  to  $3 \times 10^5$  for 100 different realizations.

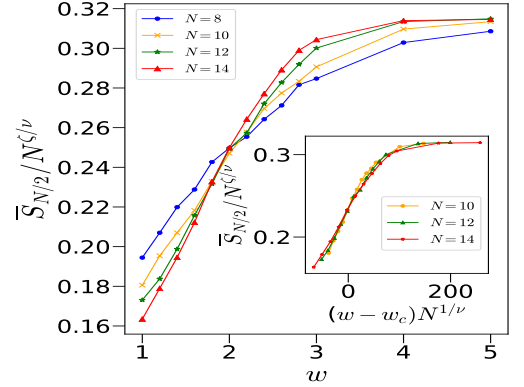


FIG. 8. (a) Plot of  $\bar{S}_{N/2} / N^{\zeta/\nu}$  vs  $w$  for  $k = 1$  corresponding to different system sizes cross each other at  $w = w_c \sim 1.8$ . Inset shows the collapse of the data with  $\nu = 0.67$  and  $\zeta = 0.76$ .

regions in these cases, we could not observe scaling behaviour. This may be attributed to the small values of angular quantum number  $j$  (proportional to system size), that we are forced to restrict ourselves to, as well as the complexity of mixed phase space (see for example [91] for cases when the initial state in a kicked top is at the border between chaos and regular regions) and the influence of phenomena such as chaos assisted tunneling [92–94], that warrants a detailed separate study.

## B. Nongeneric initial states

The above calculations were performed for a generic initial state specified by a  $(\theta, \phi)$  which has no special significance. It is interesting to study the effect of changing this initial state on the nonequilibrium dynamics and on the critical behavior. For example, in the solvable case we found that for all initial states in the  $y-z$  plane of the Bloch sphere,  $\langle J^2(n) \rangle$  eventually saturates to the RMT value, independent of the strength of the disorder. Figure 9 shows the scaling of the saturation value  $\langle J^2 \rangle$  for four different initial coherent states (see Fig. 2 for their location in phase space), including  $(\pi/2, \pi/2)$ ,  $(\pi/2, 0)$ , and two others  $(\theta, \phi) = (\pi/2, 1.9)$ ,  $(\theta, \phi) = (\pi/2, -0.56)$ , which are somewhat close to  $(\pi/2, \pi/2)$  and  $(\pi/2, 0)$ , re-

spectively. We observe a shift in  $w_c$  for certain initial states as compared to the one reported in table I.

To understand this initial state dependence behavior better, at least qualitatively, let us start from an initial state given by  $(\theta, \phi) = (\pi/2, \pi/2)$ , which is an eigenstate of  $\sigma_y$ , so that the many body state from Eq. 5 is fully delocalized along the  $x$ -direction, in which the Hamiltonian has both the interaction and the disorder. In other words the quantum coherence, as measured by the off-diagonal matrix elements of the initial state is the largest possible in the  $\sigma^x$  basis. Several recent studies have shown the importance of initial state coherence as a resource for the process of thermalization [95–97]. Thus these initial states with large coherence tend to delocalize preferentially. In the absence of disorder, the classical limit corresponding to these initial states, for  $k = 1$ , are stable fixed points, and it is interesting that the quantum effects of disorder tend to preferentially *delocalize* these states. This is consistent with a lower value of the critical strength  $w_c$  of the disorder. However, the crossing points in Fig. 9 are drifting most significantly in this case towards smaller values of  $w_c$  as  $N$  increases, and the scaling does not seem to work well. But with the system sizes we are able to go to,  $w_c$  is not larger than  $\approx 1.2$ .

On the other hand when  $(\theta, \phi) = (\pi/2, 0)$ , the initial state is an eigenstate of  $\sigma_x$ , with no off-diagonal matrix elements in  $\sigma^x$  basis, or zero quantum coherence. In this case, stronger disorder along the  $x$  interaction direction is required to equilibrate in the full Hilbert space. The scaling behavior seems to be more convincing as well, and the critical disorder strength  $w_c$  is not larger than  $\approx 2.1$ . Classically this corresponds still to a stable point, however, there is a small resonance island with nearby unstable points. Thus, the coherence of the initial states seems to play a crucial role when the dynamics is regular. We have numerically verified this argument using other values of  $(\theta, \phi)$  as well. The initial states with  $(\theta, \phi)$  closer to the  $(\pi/2, 0)$  has a larger  $w_c$  as compared to the ones closer to  $(\pi/2, \pi/2)$ , but with similar critical exponents, as shown in Fig. 9 c, d.

#### IV. CONCLUSION

In summary, this work point towards the existence of a critical strength of disorder at which there is a second order phase transition from area law entangled states with total angular momentum scaling as  $N$ , to volume law entangled states with total angular momentum scaling as  $\sqrt{N}$ . The critical disorder strength shows clear dependence on the dynamics being regular or chaotic in the disorder-free permutation symmetric space. The exponents on the other hand seem to show a weaker dependence. Most of the initial states that we checked do show a good finite size scaling behavior with roughly the same exponents as mentioned in Table I. We also understand the importance of finite sizes in these studies which may effect the results in the thermodynamic limit.

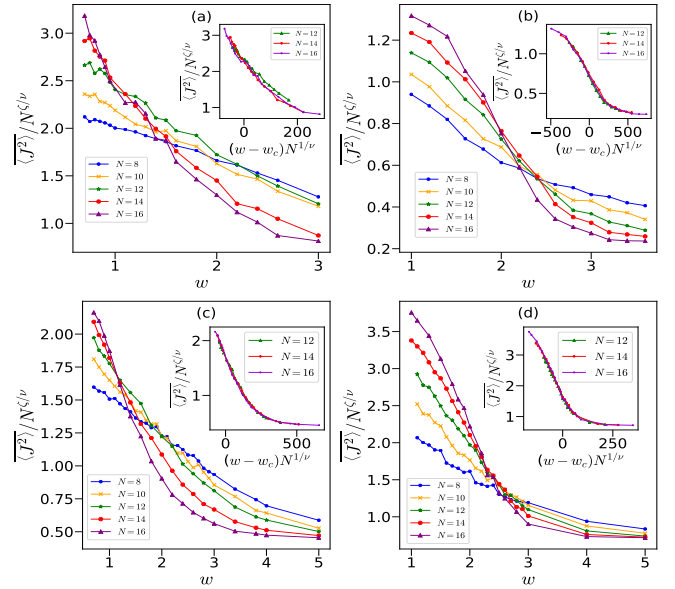


FIG. 9. Finite size scaling for  $k = 1$  and different initial conditions  $|\theta, \phi\rangle$ : (a)  $|\pi/2, \pi/2\rangle$  shows  $w_c = 1.2$ ,  $\nu = 0.55$  and  $\zeta = 0.58$ , (b)  $|\pi/2, 0\rangle$  with  $w_c = 2.1$ ,  $\nu = 0.66$  and  $\zeta = 0.47$ , (c)  $|\pi/2, 1.9\rangle$ , with  $w_c = 1.1$ ,  $\nu = 0.54$  and  $\zeta = 0.64$ . This initial condition is closer to  $(\pi/2, \pi/2)$ , and hence has a smaller  $w_c$ , (d)  $|\pi/2, -0.56\rangle$  with  $w_c = 2.3$ ,  $\nu = 0.57$  and  $\zeta = 0.58$  is similar to Fig. 6, since both the initial states are closer to  $(\pi/2, 0)$ .

From an applications perspective, our results show that for disorder less than the critical strength, permutation symmetric systems are likely to be reliably used for their intended application, being at least not volume law entangled in the full Hilbert space. It is possible that the proposed phase transition be experimentally verified by extending few qubit experimental kicked top studies [52–54], wherein disorder is anyway present. In fact, a disordered all-to-all interacting system, simulating the SYK model, has been recently experimentally studied using a combination of atomic cloud in a cavity and controllable light shift in the large detuning limit [98].

Among future directions, it will be interesting to explore if breaking permutation symmetry through other methods, say by introducing a power law interaction such as in [99], will also exhibit a similar phase transition as induced by disorder.

#### ACKNOWLEDGEMENTS

MC and UD acknowledge the HPC facility Chandra at IIT Palakkad where the computations were carried out. AL thanks Sylvia Pappalardi for discussions at an early stage of this work, at the program on “Dynamical Foundations of Many-Body Chaos”, Institut Pascal, Université Paris-Saclay, during March-April 2023, whose organizers are also gratefully acknowledged. Funding support

from the Department of Science and Technology, Govt. of India, under Grant No. DST/ICPS/QuST/Theme-

3/2019/Q69 and MPhasis for supporting the CQuiCC center are gratefully acknowledged by AL.

- 
- [1] M. Tabor, *Chaos and Integrability in Nonlinear Dynamics: An Introduction* (1989).
  - [2] A. Lichtenberg and M. Lieberman, *Regular and Chaotic Dynamics*, Applied Mathematical Sciences (Springer New York, 2013).
  - [3] E. Ott, *Chaos in Dynamical Systems*, 2nd ed. (Cambridge University Press, 2002).
  - [4] M. Gutzwiller, *Chaos in Classical and Quantum Mechanics*, Interdisciplinary Applied Mathematics (Springer New York, 1991).
  - [5] H.-J. Stöckmann, *Quantum Chaos: An Introduction* (Cambridge University Press, 1999).
  - [6] M. Mehta, *Random Matrices*, Pure and applied mathematics No. v. 142 (Elsevier/Academic Press, 2004).
  - [7] S. Wimberger, *Non Linear dynamics and Quantum Chaos - An Introduction* (Springer International Publishing Switzerland, 2014).
  - [8] L. D'Alessio, Y. Kafri, A. Polkovnikov, and M. Rigol, *Advances in Physics* **65**, 239 (2016).
  - [9] A. M. Kaufman, M. E. Tai, A. Lukin, M. Rispoli, R. Schittko, P. M. Preiss, and M. Greiner, *Science* **353**, 794 (2016).
  - [10] O. Bohigas, M. J. Giannoni, and C. Schmit, *Phys. Rev. Lett.* **52**, 1 (1984).
  - [11] M. Srednicki, *Physical Review E* **50**, 888 (1994).
  - [12] R. B. Griffiths, *Phys. Rev. Lett.* **23**, 17 (1969).
  - [13] P. W. Anderson, *Phys. Rev.* **109**, 1492 (1958).
  - [14] D. Basko, I. Aleiner, and B. Altshuler, *Annals of Physics* **321**, 1126 (2006).
  - [15] V. Oganesyan and D. A. Huse, *Phys. Rev. B* **75**, 155111 (2007).
  - [16] S. Sachdev and J. Ye, *Phys. Rev. Lett.* **70**, 3339 (1993).
  - [17] A. Kitaev, "A simple model of quantum holography (part 2), 2015," .
  - [18] J. Maldacena and D. Stanford, *Physical Review D* **94**, 106002 (2016).
  - [19] D. R. Grempel, R. E. Prange, and S. Fishman, *Phys. Rev. A* **29**, 1639 (1984).
  - [20] J. Koch, T. M. Yu, J. Gambetta, A. A. Houck, D. I. Schuster, J. Majer, A. Blais, M. H. Devoret, S. M. Girvin, and R. J. Schoelkopf, *Phys. Rev. A* **76**, 042319 (2007).
  - [21] R. Barends, J. Kelly, A. Megrant, D. Sank, E. Jeffrey, Y. Chen, Y. Yin, B. Chiaro, J. Mutus, C. Neill, P. O'Malley, P. Roushan, J. Wenner, T. C. White, A. N. Cleland, and J. M. Martinis, *Phys. Rev. Lett.* **111**, 080502 (2013).
  - [22] C. Wang, X. Li, H. Xu, Z. Li, J. Wang, Z. Yang, Z. Mi, X. Liang, T. Su, C. Yang, *et al.*, *npj Quantum Information* **8**, 3 (2022).
  - [23] C. Berke, E. Varvelis, S. Trebst, A. Altland, and D. P. DiVincenzo, *Nature Communications* **13**, 2495 (2022).
  - [24] W. Zurek, in *Time And Matter* (World Scientific, 2006) pp. 132–132.
  - [25] P. Hauke, F. M. Cucchietti, L. Tagliacozzo, I. Deutsch, and M. Lewenstein, *Reports on Progress in Physics* **75**, 082401 (2012).
  - [26] J. N. Bandyopadhyay and A. Lakshminarayan, *Physical Review Letters* **89**, 060402 (2002).
  - [27] J. Gong and P. Brumer, *Physical Review A* **68**, 022101 (2003).
  - [28] V. V. Flambaum, *Australian Journal of Physics* **53**, 489 (2000).
  - [29] P. H. Song and D. L. Shepelyansky, *Physical Review Letters* **86**, 2162 (2001).
  - [30] B. Georgeot and D. L. Shepelyansky, *Physical Review E* **62**, 6366 (2000).
  - [31] D. Braun, *Physical Review A* **65**, 042317 (2002).
  - [32] V. Madhok, S. Dogra, and A. Lakshminarayan, *Optics Communications* **420**, 189 (2018).
  - [33] D. Shepelyansky, *Physica Scripta* **2001**, 112 (2001).
  - [34] A. Piga, M. Lewenstein, and J. Q. Quach, *Physical Review E* **99**, 032213 (2019).
  - [35] K. Chinni, P. M. Poggi, and I. H. Deutsch, *Physical Review Research* **3**, 033145 (2021).
  - [36] A. Leroise and S. Pappalardi, *Physical Review A* **102**, 032404 (2020).
  - [37] Y. Braiman, J. F. Lindner, and W. L. Ditto, *Nature* **378**, 465 (1995).
  - [38] M. Lee, T. R. Look, S. P. Lim, and D. N. Sheng, *Phys. Rev. B* **96**, 075146 (2017).
  - [39] A. Pal and D. A. Huse, *Phys. Rev. B* **82**, 174411 (2010).
  - [40] D. J. Luitz, N. Laflorencie, and F. Alet, *Phys. Rev. B* **91**, 081103 (2015).
  - [41] A. Seshadri, V. Madhok, and A. Lakshminarayan, *Physical Review E* **98**, 052205 (2018).
  - [42] M. O. Scully, *Physical Review Letters* **115**, 243602 (2015).
  - [43] M. Gegg, A. Carmele, A. Knorr, and M. Richter, *New Journal of Physics* **20**, 013006 (2018).
  - [44] O. Rubies-Bigorda and S. F. Yelin, *Physical Review A* **106**, 053717 (2022).
  - [45] Z. Qi, T. Scaffidi, and X. Cao, *Phys. Rev. B* **108**, 054301 (2023).
  - [46] F. Iemini, D. Chang, and J. Marino, *Phys. Rev. A* **109**, 032204 (2024).
  - [47] F. Haake, M. Kuś, and R. Scharf, *Zeitschrift für Physik B Condensed Matter* **65**, 381 (1987).
  - [48] G. M. D'Ariano, L. R. Evangelista, and M. Saraceno, *Phys. Rev. A* **45**, 3646 (1992).
  - [49] F. Haake, S. Gnutzmann, and M. Kuś, *Quantum Signatures of Chaos*, Springer complexity (Springer, 2018).
  - [50] X. Wang, S. Ghose, B. C. Sanders, and B. Hu, *Physical Review E* **70**, 016217 (2004).
  - [51] V. Madhok, V. Gupta, D.-A. Trottier, and S. Ghose, *Physical Review E* **91**, 032906 (2015).
  - [52] S. Chaudhury, A. Smith, B. Anderson, S. Ghose, and P. S. Jessen, *Nature* **461**, 768 (2009).
  - [53] C. Neill, P. Roushan, M. Fang, Y. Chen, M. Kolodrubetz, Z. Chen, A. Megrant, R. Barends, B. Campbell, B. Chiaro, A. Dunsworth, E. Jeffrey, J. Kelly, J. Mutus, P. J. J. O'Malley, C. Quintana, D. Sank, A. Vainsencher, J. Wenner, T. C. White, A. Polkovnikov, and J. M. Martinis, *Nature Physics* **12**, 1037 (2016).



- [54] V. Krithika, V. Anjusha, U. T. Bhosale, and T. Mahesh, *Physical Review E* **99**, 032219 (2019).
- [55] K. Zyczkowski, *Journal of Physics A: Mathematical and General* **23**, 4427 (1990).
- [56] B. Sanders and G. Milburn, *Zeitschrift für Physik B Condensed Matter* **77**, 497 (1989).
- [57] U. T. Bhosale and M. Santhanam, *Physical Review E* **98**, 052228 (2018).
- [58] R. F. Fox and T. C. Elston, *Physical Review E* **50**, 2553 (1994).
- [59] X. Wang, J. Ma, L. Song, X. Zhang, and X. Wang, *Physical Review E* **82**, 056205 (2010).
- [60] Z. Zou and J. Wang, *Entropy* **24**, 1092 (2022).
- [61] M. H. Muñoz-Arias, P. M. Poggi, and I. H. Deutsch, *Physical Review E* **103**, 052212 (2021).
- [62] L. J. Fiderer and D. Braun, *Nature Communications* **9**, 1351 (2018).
- [63] U. T. Bhosale and M. Santhanam, *Physical Review E* **95**, 012216 (2017).
- [64] L. M. Sieberer, T. Olsacher, A. Elben, M. Heyl, P. Hauke, F. Haake, and P. Zoller, *npj Quantum Information* **5**, 78 (2019).
- [65] M. Kumari and S. Ghose, *Phys. Rev. E* **97**, 052209 (2018).
- [66] M. Lombardi and A. Matzkin, *Physical Review E* **83**, 016207 (2011).
- [67] A. Anand, J. Davis, and S. Ghose, *Phys. Rev. Res.* **6**, 023120 (2024).
- [68] S. Ghose, R. Stock, P. Jessen, R. Lal, and A. Silberfarb, *Physical Review A* **78**, 042318 (2008).
- [69] N. Defenu, T. Donner, T. Macrì, G. Pagano, S. Ruffo, and A. Trombettoni, *Rev. Mod. Phys.* **95**, 035002 (2023).
- [70] N. Defenu, A. Leroze, and S. Pappalardi, *Physics Reports* **1074**, 1 (2024).
- [71] S. Pappalardi, A. Russomanno, B. Žunkovič, F. Iemini, A. Silva, and R. Fazio, *Physical Review B* **98**, 134303 (2018).
- [72] V. Constantoudis and N. Theodorakopoulos, *Physical Review E* **56**, 5189 (1997).
- [73] Q. Wang and M. Robnik, *Entropy* **23**, 1347 (2021).
- [74] R. J. Glauber and F. Haake, *Physical Review A* **13**, 357 (1976).
- [75] Y. Lee Loh and M. Kim, *American Journal of Physics* **83**, 30 (2015).
- [76] R. Puri, *Mathematical Methods of Quantum Optics* (Springer Berlin, 2001).
- [77] J. B. Ruebeck, J. Lin, and A. K. Pattanayak, *Physical Review E* **95**, 062222 (2017).
- [78] S. Dogra, V. Madhok, and A. Lakshminarayan, *Physical Review E* **99**, 062217 (2019).
- [79] P. Sreeram, V. Madhok, and A. Lakshminarayan, *Journal of Physics D: Applied Physics* **54**, 274004 (2021).
- [80] O. A. Castro-Alvaredo and B. Doyon, *Journal of Statistical Mechanics: Theory and Experiment* **2013**, P02016 (2013).
- [81] D. N. Page, *Physical Review Letters* **71**, 1291 (1993).
- [82] A. Young, *Physical Review E* **96**, 032112 (2017).
- [83] D. Thirumalai, Q. Li, and T. Kirkpatrick, *Journal of Physics A: Mathematical and General* **22**, 3339 (1989).
- [84] S. Pappalardi, A. Polkovnikov, and A. Silva, *SciPost Phys.* **9**, 021 (2020).
- [85] R. Botet, R. Jullien, and P. Pfeuty, *Phys. Rev. Lett.* **49**, 478 (1982).
- [86] R. Botet and R. Jullien, *Phys. Rev. B* **28**, 3955 (1983).
- [87] B. Skinner, J. Ruhman, and A. Nahum, *Phys. Rev. X* **9**, 031009 (2019).
- [88] Y. Li, X. Chen, and M. P. A. Fisher, *Phys. Rev. B* **98**, 205136 (2018).
- [89] J. Cardy, *Finite-size Scaling*, Current physics (North-Holland, 1988).
- [90] Y. Wang, C. Cheng, X.-J. Liu, and D. Yu, *Phys. Rev. Lett.* **126**, 080602 (2021).
- [91] V. Madhok, *Phys. Rev. E* **92**, 036901 (2015).
- [92] S. Tomsovic and D. Ullmo, *Phys. Rev. E* **50**, 145 (1994).
- [93] S. Keshavamurthy and P. Schlagheck, *Dynamical Tunneling: Theory and Experiment* (CRC Press, Boca Raton, FL, 2011).
- [94] V. R. Krithika, M. S. Santhanam, and T. S. Mahesh, *Phys. Rev. A* **108**, 032207 (2023).
- [95] G. Styliaris, N. Anand, L. Campos Venuti, and P. Zanardi, *Phys. Rev. B* **100**, 224204 (2019).
- [96] J. J. Pulikkottil, A. Lakshminarayan, S. C. L. Srivastava, M. F. I. Kieler, A. Bäcker, and S. Tomsovic, *Phys. Rev. E* **107**, 024124 (2023).
- [97] A. Mitra and S. C. L. Srivastava, *Phys. Rev. E* **108**, 054114 (2023).
- [98] N. Sauerwein, F. Orsi, P. Uhrich, S. Bandyopadhyay, F. Mattiotti, T. Cantat-Moltrecht, G. Pupillo, P. Hauke, and J.-P. Brantut, *Nature Physics* **19**, 1128 (2023).
- [99] A. Russomanno, M. Fava, and M. Heyl, *Physical Review B* **104**, 094309 (2021).